Title

Crimp Induced Leaflet Damage and Calcification of Transcatheter Heart Valves

Permalink

https://escholarship.org/uc/item/6qw6g8mb

Journal

CARDIOLOGY, 134(2)

ISSN

0008-6312

Authors

Sinha, Aditi
Barannyk, Oleksandr
Kheradvar, Arash

Publication Date

2016

Peer reviewed

Effect of stent crimping on calcification of transcatheter aortic valves

Ramin Zareian[a], Jen-Chieh Tseng[b], Robert Fraser[c], Jeffrey Meganck[b], Marshall Kilduff[c],
Mohammad Sarraf[d], Danny Dvir[e] and Arash Kheradvar[a,*]

[a] The Edwards Lifesciences Center for Advanced Cardiovascular Technology, University of California Irvine, Irvine, CA, USA
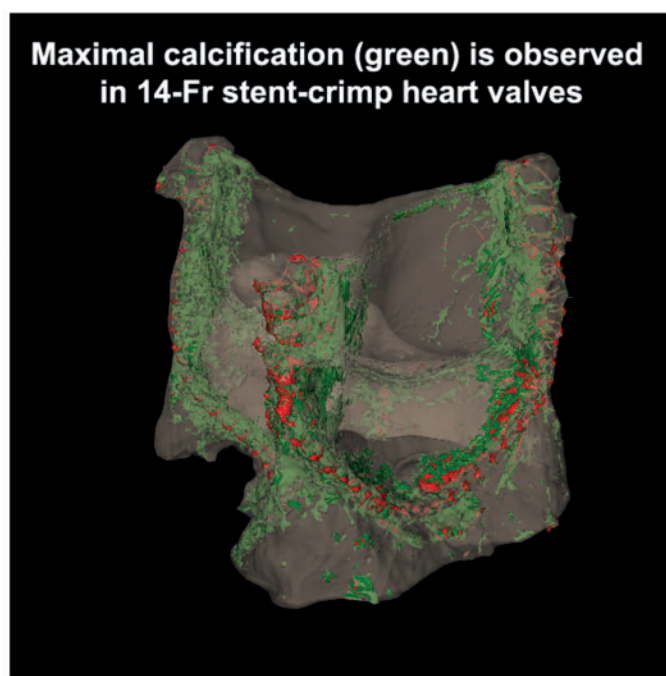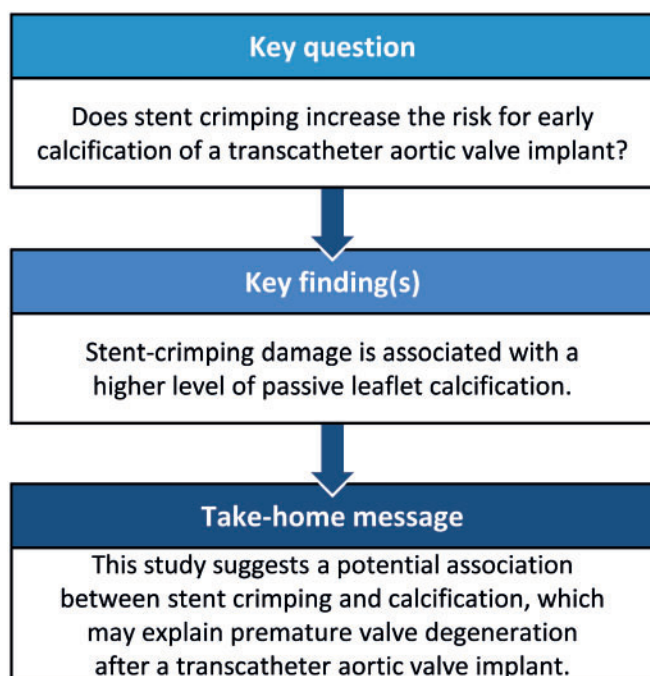[b] PerkinElmer Inc., Hopkinton, MA, USA
[c] ViVitro Labs Inc., Victoria, BC, Canada
[d] Cardiovascular Division, University of Alabama at Birmingham, Birmingham, AL, USA
[e] Division of Cardiology, University of Washington Medical Center, Seattle, WA, USA

* Correspondence author: Departments of Biomedical Engineering, and Medicine (Cardiology), Edwards Lifesciences Center for Advanced Cardiovascular Technology, University of California Irvine, 2410 Engineering Hall, Irvine, CA 92697-2730, USA. Tel: +1-949-8246538; fax: +1-949-8249968; e-mail: arashkh@uci.edu (A. Kheradvar).

Key question

Does stent crimping increase the risk for early calcification of a transcatheter aortic valve implant?

Key finding(s)

Stent-crimping damage is associated with a higher level of passive leaflet calcification.

Take-home message

This study suggests a potential association between stent crimping and calcification, which may explain premature valve degeneration after a transcatheter aortic valve implant.

Maximal calcification (green) is observed in 14-Fr stent-crimp heart valves

Abstract

OBJECTIVES: Although many challenges related to the acute implantation of transcatheter aortic valves have been resolved, durability and early degeneration are currently the main concerns. Recent reports indicate the potential for early valve degeneration and calcification. However, only little is known about the underlying mechanisms behind the early degeneration of these valves. The goal of this study was to test whether stent crimping increases the risk for early calcification.

METHODS: Stented valves that were crimped at 18-Fr and 14-Fr catheter and uncrimped controls were exposed to a standard calcifying solution for 50 million cycles in an accelerated wear test system. Subsequently, the leaflets of the valves were imaged by microcomputed tomography (micro-CT) followed by histochemical staining and microscopic analyses to quantify calcification and other changes in the leaflets' characteristics.

RESULTS: Heavily calcified regions were found over the stent-crimped leaflets compared to uncrimped controls, particularly around the stent's struts. Micro-CT studies measured the total volume of calcification in the uncrimped valves as $77.31 \pm 1.63 \, mm^3$ vs $95.32 \pm 5.20 \, mm^3$

in 18-Fr and 110.01 ± 8.33 mm^3 in 14-Fr stent-crimped valves, respectively. These results were congruent with the increase in leaflet thickness measured by CT scans (0.44 ± 0.07 mm in uncrimped valves vs 0.69 ± 0.15 mm and 0.75 ± 0.09 mm in 18-Fr and 14-Fr stent-crimped valves, respectively). Histological studies confirmed the micro-CT results, denoting that the percentage of calcification in uncrimped leaflets at the valve's posts was 5.34 ± 3.97 compared to 19.97 ± 6.18 and 27.64 ± 13.17 in the 18-Fr and 14-Fr stent-crimped leaflets, respectively.

CONCLUSIONS: This study concludes that stent-crimping damage is associated with a higher level of passive leaflet calcification, which may contribute to early valve degeneration.

Keywords: Transcatheter aortic valve • Calcification • Degeneration • Stent-crimp

INTRODUCTION

Transcatheter aortic valve replacement (TAVR) is an emerging technology with great promise for revolutionizing the treatment of valvular heart disease. Short-term data suggest that TAVR in patients with severe aortic stenosis who were unsuitable candidates for surgery significantly reduces all-cause mortality, the composite end point of all-cause death and repeat hospitalization and cardiac symptoms, compared to standard therapy, with a comparable incidence of stroke and major vascular events. More recent studies suggest that TAVR provides patients with an intermediate risk for traditional surgery a similar outcome with respect to the primary end point of death or disabling stroke at 2 years [1]. However, because TAVR has only been widely available since 2007, its long-term durability is not yet known [2].

Transcatheter heart valves share some characteristics with bioprosthetic surgical valves but also have many unique properties [3]. The most important similarity is their leaflet, which is made mainly of pericardial tissue. Alternatively, their major difference is the housing of the transcatheter heart valve leaflets within a stent, exposure to stent crimping before implantation and non-optimal expansion, which may lead to unfavourable interaction with the native aortic root. The design of these valves leaves the pericardial leaflets crimped within a compressed stent during delivery until implantation, which takes about 5–10 min. Doing so exposes the stented leaflets to a level of stress that is not applied to surgical bioprosthetic valves. Currently, only minimal quantitative data are available on the basis of which to assess the damage that results from stent crimping [4–6]. More recently, several clinical studies have reported premature degeneration of the transcatheter heart valves [7–14]. However, no quantitative study has yet convincingly shown that stent crimp-induced damage to the leaflets is indeed the reason for premature structural degeneration and calcification. Further, these areas could be a nidus for valve leaflet thrombosis, which is known to be more common in TAVR [15]. The goal of this study was to test the effect of stent crimping on premature calcification.

MATERIALS AND METHODS

Seven 25-mm self-expandable heart valves were developed, each having a nitinol stent with leaflets made of clinical-quality bovine pericardial tissue (XenoSure Biologic Patch, LeMaitre Vascular, Burlington, MA, USA). The durability experiment was performed using a standard accelerated wear test (AWT) system (HiCycle Durability Tester, ViVitro Inc., Victoria, BC, Canada) that can accommodate up to 6 heart valves. Among the 7 valves, 4 were crimped and held at 18-Fr (n = 2) and 14-Fr (n = 2) for 5 min with the valves' leaflets inside the stent; 2 valves were kept uncrimped

and used as the control for the AWT in the presence of the calcifying solution, as described by Barannyk *et al.* [16]. The last valve was kept intact as a control for imaging and histological studies. Testing in the presence of a calcifying solution is the industry standard to determine the calcification potential of the heart valves and shows the tendency of the valves to passive calcification [17, 18] (Fig. 1).

Crimping the stented aortic valves

The transcatheter aortic valves were divided into 4 different groups: group 0 (control uncrimped, N = 1), group 1 (uncrimped calcified, N = 2), group 2 (crimped at 18-Fr calcified, N = 2) and group 3 (crimped at 14-Fr and calcified, N = 2). The valves in groups 0 and 1 remained uncrimped, and valves in groups 2 and 3 were crimped at 18-Fr and 14-Fr, respectively. A standard valve crimper was used to crimp the valves in groups 2 and 3. Prior to crimping, all valves in groups 2 and 3 were first immersed in warm water (∼37°C) for 30 min to attain the nitinol stent's full diameter. Finally, all 6 valves in groups 1–3 were placed in saline and shipped to ViVitro Labs for AWT.

50-million cycle accelerated wear test

All 6 valves in groups 1–3 were placed in silicone test fixtures with an inner diameter of 24 mm. These fixtures were fabricated from GI-1040 silicone (Silicones, Inc., High Point, NC, USA) and had a durometer of Shore A 40. This hardness was selected to match the tissue properties of a calcified aortic annulus. To
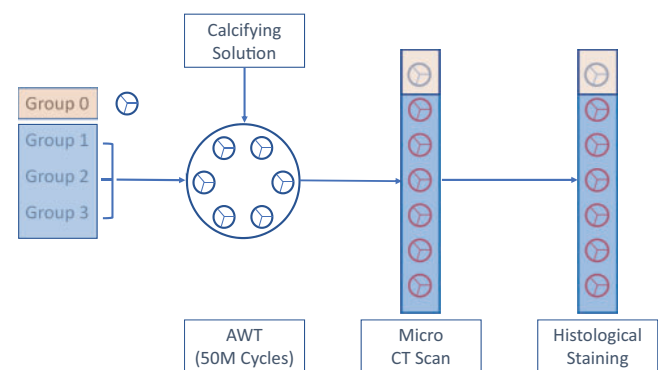

Figure 1: Schematics of the experiments to quantify and compare the durability of heart valves. The diagram shows the 6 valves in groups 1–3 that are tested for durability in the presence of a calcifying solution and then compared with alike control valve in group 0 by microcomputed tomography scans and histological staining. Group 0: control; uncrimped (N = 1); group 1: uncrimped calcified (N = 2); group 2: crimped at 18-Fr calcified (N = 2); and group 3: crimped at 14-Fr and calcified (N = 2). AWT: accelerated wear test; CT: computed tomography.

prevent paravalvular leakage and ensure that the valves did not migrate during the test, Dow Corning 734 Flowable RTV silicone was injected around the perimeter of the transcatheter valve to seal the perimeter to the silicone test fixture. The valves mounted in test fixtures were then placed into the ViVitro Labs' HiCycle for AWT. The valves were immersed in a calcification solution, consisting of KCl (55 mM), $CaCl_2$ (1.5 mM), KH_2PO_4 (1.25 mM) and barbital buffer (20 mM), which was maintained at 37°C for the duration of the test, as described previously [16]. Full opening and closure of the valves were achieved at 1000 cycles per minute. The peak differential pressure during the valve closure was maintained at 100 mmHg, in accordance with the aortic valve normotensive conditions defined in ISO 5840-3:2013. Testing was conducted for 50 million cycles, or nearly 34 days. This duration is equivalent to almost 15 months in a native heart. During the testing, the calcification solution was changed weekly to ensure adequate concentration of Ca^{++} and HPO_4. The concentration of calcium and phosphate was 1.2 times more than that in a normal healthy individual (1.57 $mmol^2/l^2$) and lower than high-risk level (2.24 $mmol^2/l^2$) in blood [16, 19]. The pH of the solution was measured at each fluid change and kept in a range between 7.37 and 7.46. The valves were shipped back to the University of California, Irvine in saline immediately after completion of the test for further analyses.

Quantifying the calcification by microcomputed tomographic scanning

All 7 valves were sent to PerkinElmer, Inc. to be imaged using a microcomputed tomography (micro-CT) system (Quantum GX2; PerkinElmer, Hopkinton, MA, USA). A similar acquisition setting was used for scanning all the valves: 90 KV, 88 μA; field of view: 36 mm; acquisition time: 14 min; camera mode: high resolution. A subvolume reconstruction of the original images with a field of view of 10 mm and a voxel size of 20 μm was performed to obtain higher resolution data of the valves' leaflets to detect and quantify calcification. All 7 valves were imaged from top to bottom (z-stack imaging) with and without their nitinol stents. All images were imported into VivoQuant 3.0 software (Invicro LLC, Boston, MA, USA) to quantify and distinguish the sutures and calcification regions, respectively.

Quantifying the valve thickness

The transverse view (top view) of all the valves (groups 0–3) were imported into the VivoQuant software. The leaflet of each valve was measured adjacent to the valve's posts and at the centre of the leaflet's belly. In total, the leaflet thickness was measured at 9 positions for each valve.

Quantifying the calcification by histological analyses

To validate the CT scan analyses after completion of the imaging studies, the valves' leaflets were carefully detached from the stents for histological analyses. Three tissue cross-sections (3 mm diameter) were collected from each valve's posts near the stent using a biopsy punch (3 specimens for each valve). All specimens were stored in saline and shipped to North Bay Histology Lab (Novato, CA, USA) for analyses. Each sample was individually embedded, sectioned and stained for calcium characterization (Von Kossa stain), elastin composition (Verhoeff-van Gieson stain) and collagen fibre quantification (trichrome III and haematoxylin and eosin stains). The stained samples were visualized using a light microscope and stored as digital computer images for further analyses. From each stained sample, more than 10 images were captured and stitched together to reconstruct the complete field of view of the tissue cross-section.

The images acquired from the Von Kossa-stained sample were imported into a computer, and an in-house MATLAB (MathWorks, Inc., Natick, MA, USA) routine was used to analyse the data. The total pixels for each image were first calculated and quantified in red, green and blue values, and the calcified and uncalcified pixels were assigned to red and blue values in reconstructed images, respectively. Finally, the ratio of calcified pixels with respect to the total pixels (the total calcified and uncalcified pixels) in terms of percentage was calculated and plotted.

Statistical analysis

All the data quantified from the micro-CT scan and histological samples are presented as mean ± standard deviation. Because only 6 valves could be loaded for each AWT experiment, the number of our samples for each study group was small. Therefore, to analyse the data, each study group was compared using a non-parametric test (Mann–Whitney U-test) [20]. The $U_{Critical}$ for each pairwise comparison was determined from the Mann–Whitney U-test table (2-tailed testing) based on a 2-sided level of significance ($\alpha = 0.05$). The minimum of the calculated U for each pairwise comparison was compared to the $U_{Critical}$. Based on the Mann–Whitney U-test, if the minimum calculated U was less than or equal to the $U_{Critical}$, the null hypothesis (indistinguishable trait in 2 studied groups) was rejected in favour of the research hypothesis (distinct trait in 2 studied groups). If the U was greater than the $U_{Critical}$, the null hypotheses could not be rejected; thus, there was no difference between the 2 studied groups. Due to the small sample size in this study, we only report the U values and compare the $U_{Minimum}$ to $U_{Critical}$ for each studied group.

RESULTS

Microcomputed tomographic imaging results

Quantification of valve calcification. The leaflet calcification is compared among the different groups in Fig. 2. The sutures and calcification regions are distinguished by red and green, respectively. Figure 3C and D compare the total measured calcification among the studied groups. The total volume of calcification in the uncrimped valves was 77.31 ± 1.63 mm^3 vs 95.32 ± 5.20 mm^3 for 18-Fr and 110.01 ± 8.33 mm^3 for 14-Fr stent-crimped, respectively. Based on the pairwise non-parametric analyses, the volume of calcification in the uncrimped valves ($N = 2$) was less than that in the crimped valves at 18-Fr ($N = 2$) and at 14-Fr ($N = 2$); as well, this quantity was different between both crimped groups (Mann–Whitney $U_{Minimum} = 0$, $n_2 = n_3 = n_4 = 2$).

Any increase to the suture volume beyond the baseline value after the 50-million cycle test was attributed to the deposition of calcium over the sutures. However, since calcification around the sutures is not related to our hypothesis considering the effect of
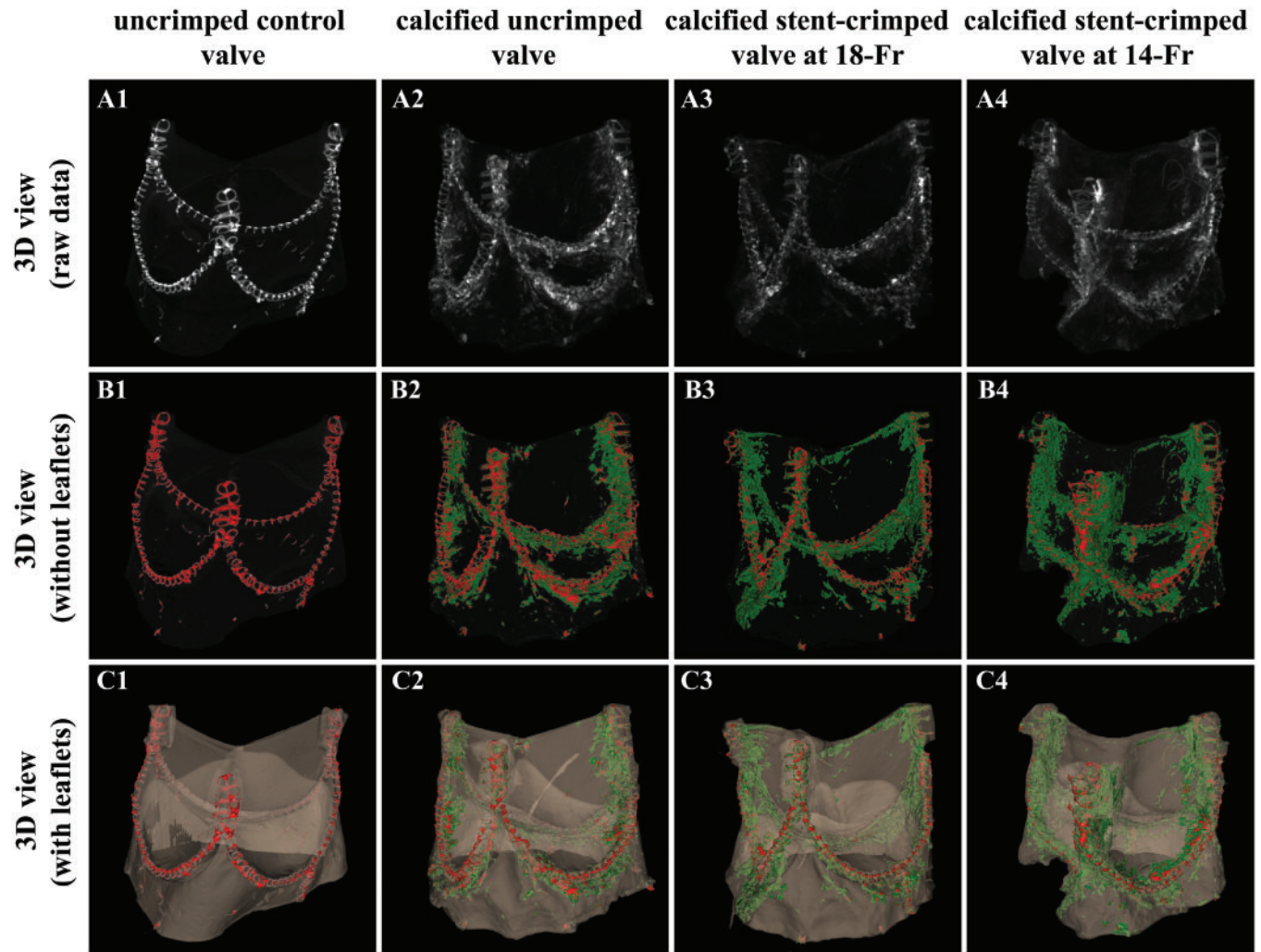
Figure 2: Comparison between stent-crimped and uncrimped valves after 50 million cycles of the accelerated wear test. The raw data representing 3D microcomputed tomographic (micro-CT) scans of an uncrimped control valve (**A1**); a calcified uncrimped valve (**A2**); a calcified stent-crimped valve at 18-Fr (**A3**); and a calcified stent-crimped valve at 14-Fr (**A4**). The 3D view of the quantified micro-CT images of an uncrimped control valve (**B1**), a calcified uncrimped valve (**B2**), a calcified stent-crimped valve at 18-Fr (**B3**) and calcified stent-crimped valve at 14-Fr (**B4**) showing the valve's sutures and calcified regions in red and green, respectively. The 3D views of the quantified micro-CT images of an uncrimped control valve (**C1**), a calcified uncrimped valve (**C2**), a calcified stent-crimped valve at 18-Fr (**C3**) and calcified stent-crimped valve at 14-Fr (**C4**) along with the valve's leaflets. 3D: 3-dimensional.

stent crimping, we did not consider that increase in volume as calcium deposition in the leaflet. Nevertheless, these changes in the volume of the sutures are reported in Fig. 3B. The volume of the baseline sutures in the control uncrimped valve was 20.38 mm^3 ($N = 1$), whereas the total volume of the sutures had increased to $47.28 \pm 0.44 \text{ mm}^3$ ($N = 2$), $43.96 \pm 6.94 \text{ mm}^3$ ($N = 2$) and $42.88 \pm 4.17 \text{ mm}^3$ ($N = 2$) for uncrimped, 18-Fr and 14-Fr crimped valves, respectively (Fig. 3B). According to the non-parametric analyses, the total volume of sutures in group 0 was different than that in groups 1–3 (Mann–Whitney $U_{Minimum} = 0$, $n_1 = 1$, $n_{2,3,4} = 6$). This finding suggests that calcium deposition occurs around the sutures in valves exposed to a calcifying solution, regardless of stent crimping.

Quantification of leaflet thickness. Following 50 million cycles of AWT, the thickness of the valve leaflets was measured at 9 different locations, as discussed previously (Fig. 4). The average thickness of the uncrimped control leaflets was $0.30 \pm 0.04 \text{ mm}$, whereas the average thickness of the uncrimped/calcified and

stent-crimped leaflets at 18-Fr and 14-Fr was $0.44 \pm 0.07 \text{ mm}$, $0.75 \pm 0.09 \text{ mm}$ and $0.69 \pm 0.15 \text{ mm}$, respectively. Figure 5B shows a comparison of the leaflet thickness among the studied groups. The average thickness of the uncrimped control leaflets differed from that of uncrimped/calcified leaflets (Mann–Whitney $U_{Minimum} = 5 < U_{Critical} = 42$, $n_1 = 9$, $n_2 = 18$). As well, the average thickness of the uncrimped/calcified leaflets differed from that of the stent-crimped leaflets at 18-Fr (Mann–Whitney $U_{Minimum} = 2 < U_{Critical} = 99$, $n_2 = 18$, $n_3 = 18$) and to stent-crimped leaflets at 14-Fr (Mann–Whitney $U_{Minimum} = 25 < U_{Critical} = 99$, $n_2 = 18$, $n_4 = 18$). Nevertheless, the average thickness of the stent-crimped leaflets at 18-Fr did not differ from that of the 14-Fr (Mann–Whitney $U_{Minimum} = 125 > U_{Critical} = 99$, $n_3 = 18$, $n_4 = 18$).

Histological results

Figure 6A1 shows the Von Kossa staining of a control uncalcified/uncrimped leaflet with cells and cytoplasm in red and pink without any calcified regions. Figure 6B1–D1 represent Von Kossa
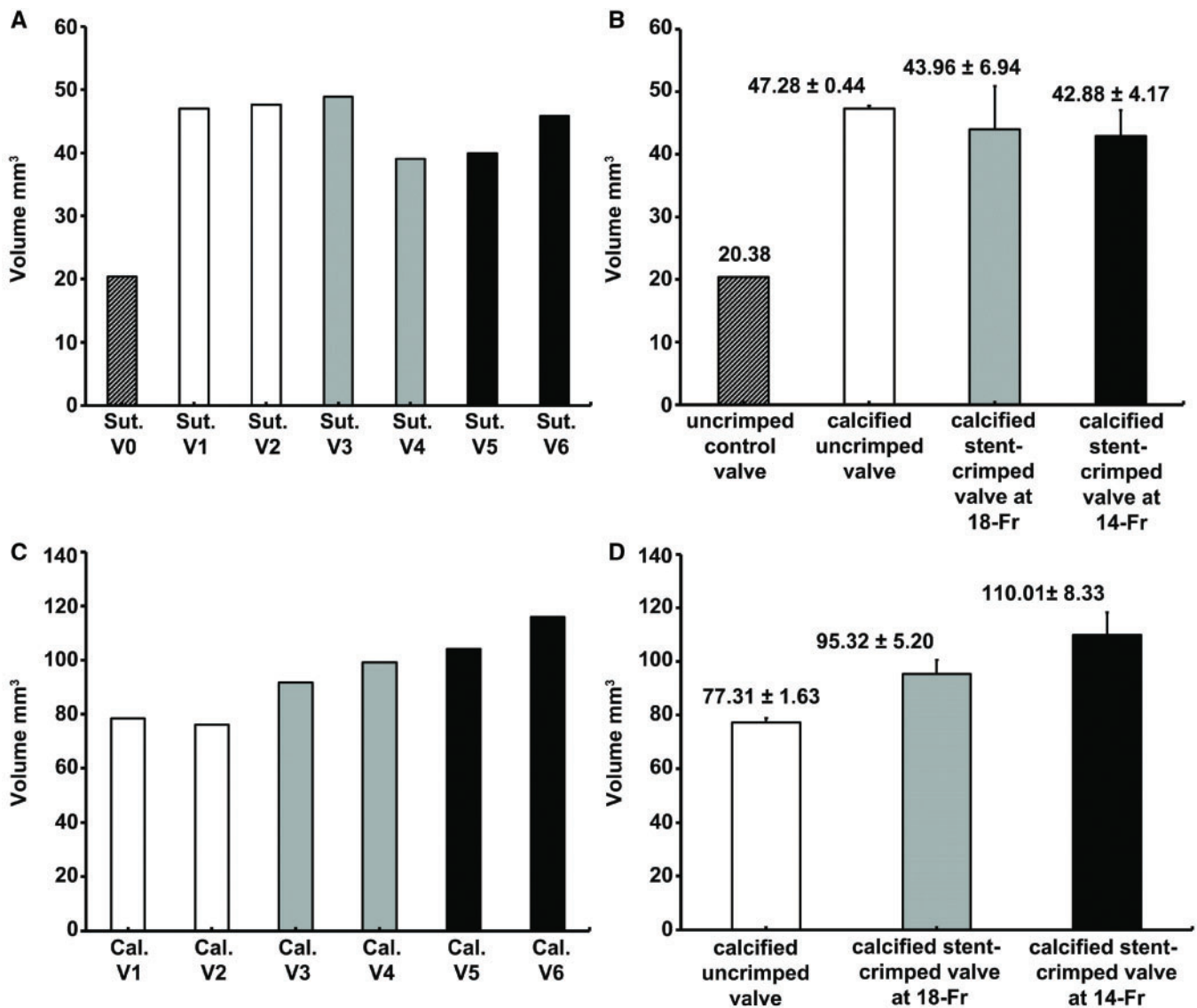
Figure 3: Quantification of calcified regions using microcomputed tomographic scanning. (**A**) Total suture volume was quantified for each valve. (**B**) The quantified suture volume for each group is shown as the mean ± standard deviation. (**C**) Total calcification volume is quantified for each valve. (**D**) The quantified calcification volume for each group is shown as mean ± standard deviation. Cal: calcification; Sut: suture; V0: (valve 0) uncrimped control; V1: (valve 1) calcified uncrimped; V2: (valve 2) calcified uncrimped; V3: (valve 3) calcified crimped valve at 18-Fr; V4: (valve 4) calcified crimped valve at 18-Fr; V5: (valve 5) calcified crimped valve at 14-Fr; V6: (valve 6) calcified crimped valve at 14-Fr.

staining of the calcified valves. The calcified regions are clearly detectable in the images as black regions (Fig. 6B1–D1), and the top and bottom tissue layers were calcified and degenerated compared to the leaflet tissue core. The uncrimped valves showed calcification in the superficial layers of their leaflets (Fig. 6B1), whereas the stent-crimped valves were deeply calcified at both the ventricular and aortic sides of the leaflets (Fig. 6C1 and D1). Subsequently, the calcified regions were quantified and measured by an in-house MATLAB code that detects and counts the pixels stained by Von Kossa. The ratio of the calcification to the whole tissue cross-section (expressed in terms of percentage) was calculated for each valve's posts and then averaged for each study group (Fig. 7A and B). The data indicate that the uncrimped leaflets showed an average calcification of 5.34 ± 3.97% vs the stent-crimped leaflets, which had an average calcification of 19.97 ± 6.18% and 27.64 ± 13.17% at 18-Fr and 14-Fr stent crimping, respectively. The non-parametric test shows that the average

calcification of the uncrimped/calcified valve compared to that of the crimped/calcified valves at 18-Fr (Mann–Whitney $U_{Minimum} = 0 < U_{Critical} = 5$, $n_2 = 6$, $n_3 = 6$) or between the uncrimped/calcified valves and the crimped/calcified valves at 14-Fr differed (Mann–Whitney $U_{Minimum} = 0 < U_{Critical} = 5$, $n_2 = 6$, $n_4 = 6$). No difference was observed between the valves crimped at 18-Fr and 14-Fr (Mann–Whitney $U_{Minimum} = 12 > U_{Critical} = 5$, $n_3 = 6$, $n_4 = 6$).

Figure 8 presents the tissue cross-sections from each valve's post, stained with trichrome, Verhoeff-van Gieson and haematoxylin and eosin. Figure 8 shows the staining of control, uncrimped, 18-Fr and 14-Fr stent-crimped valves, respectively. The cross-sections of the uncrimped leaflets show the normal structure of the cells and the extracellular matrix (ECM) (Fig. 8A1–3) with elastin and collagen fibres in pink and blue staining, respectively (Fig. 8A1–3). Figure 8B1–3, C1–3 and D1–3 demonstrate that the ECM of the calcified tissue possesses a
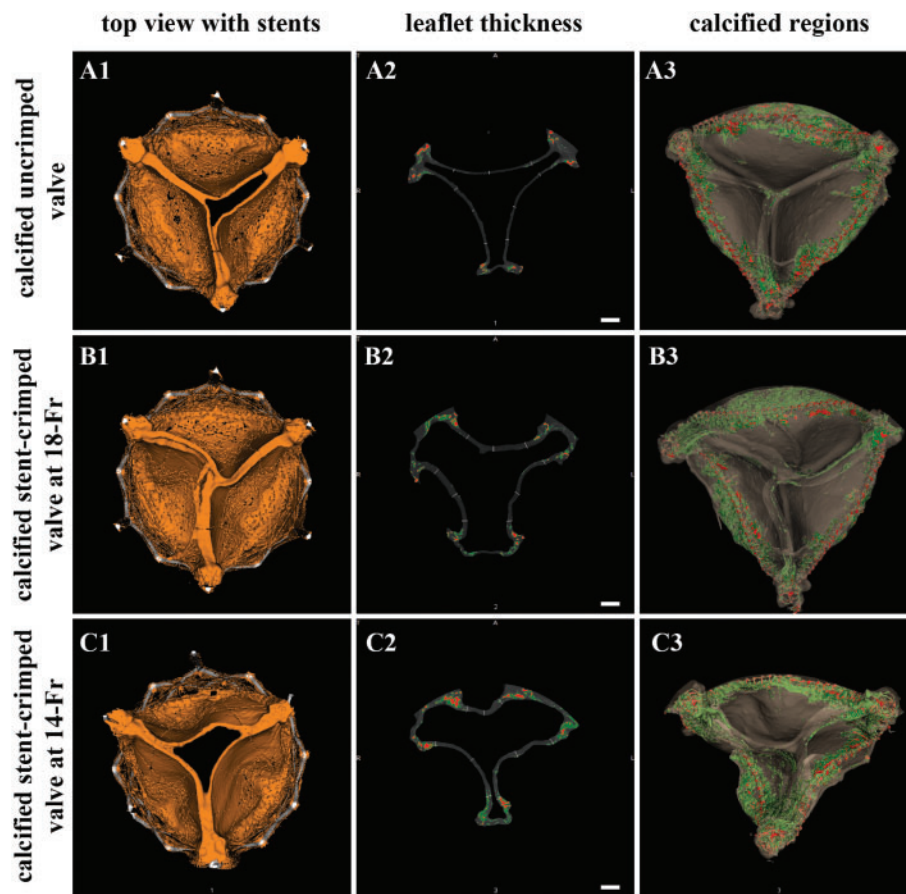
Figure 4: Association between the thickness of the leaflets and calcification. Microcomputed tomographic (micro-CT) views of a calcified uncrimped valve (**A1–3**); a calcified stent-crimped valve at 18-Fr (**B1–3**); and a calcified stent-crimped valve at 14-Fr (**C1–3**). **A1**, **B1** and **C1** show the top views of the valves; **A2**, **B2** and **C2** show how valves are quantified at each slice from the z-stack. **A3**, **B3** and **C3** show the fully analysed CT images of the valve, differentiating between sutures (red) and calcification regions (green), respectively. Scale bars are 2.5 mm.

different structure in all the studied valves, which is more pronounced at the calcified regions. The superficial layers of the leaflets show the effect of calcification on the ECM, whereas the core of the leaflets remained intact. Based on trichrome and haematoxylin and eosin staining, the calcification led to degeneration of collagen and elastin fibres at the superficial layers of the calcified heart valves. In uncrimped valves, collagen and elastin fibres were degraded only at the superficial layers of the leaflets (Fig. 8B1–3), whereas in both groups of stent-crimped valves, collagen and elastin fibres were degenerated on both the aortic and ventricular sides of the leaflets (Fig. 8C1–3 and D1–3). In these valves, degradation of the collagen and elastin advanced to the deeper tissue layers of the leaflets. Figures 6C1–D1 show that the calcified regions evolved from the superficial layers towards the tissue core.

DISCUSSION

The consensus among the experts is that the durability of surgical bioprosthetic and transcatheter valves may differ because in transcatheter valves, the leaflets mounted within the stent are prone to microscopic damage due to stent crimping [2]. In the early days of TAVR, the main focus was on the short-term procedural success. Nevertheless, the durability of the valve's leaflets becomes more relevant because TAVR is being offered to

younger and lower risk patients. These patients are expected to survive much longer than those who received TAVR in the early days. Thus, improving durability of the valve is of significant importance. We have addressed whether stent crimping of the valve leaflets is responsible for structural valve degeneration after 50 million cycles (equivalent to 15 months in the human heart) of exposure to a standard calcifying solution.

Association of stent crimping with leaflet thickening and calcification

As validated by histological analysis, our micro-CT data show that calcification is more prominent in the regions around the valve sutures and at the valves' posts (Fig. 2), which are under high mechanical stress. Stented valves crimped at 18-Fr and 14-Fr (Fig. 3D) exhibited more calcification than the uncrimped valves; however, the difference between the 2 stent-crimped valve groups was not noticeable, denoting that more aggressive crimping than 18-Fr may not lead to further passive calcification. However, because it was previously shown that more aggressive stent crimping is associated with deeper tissue damage [21], the new results should be considered with caution, and further validation with a large cohort of valves may be needed to confirm them. Furthermore, we found that the crimped leaflets (Fig. 5B) were thicker than the uncrimped leaflets after 50 million
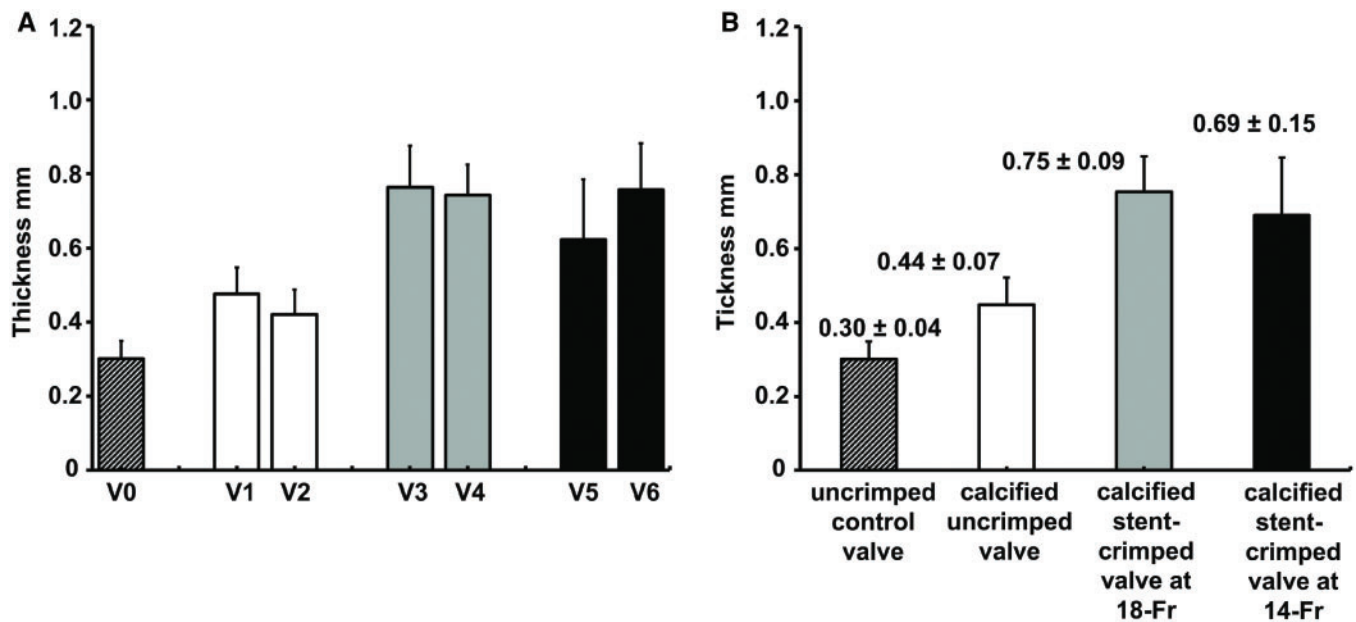
Figure 5: Valve thickness measurement using microcomputed tomographic scanning. (**A**) The measured thickness of the leaflets for each studied valve. (**B**) The measured thicknesses of the leaflets for each studied group. The measured thicknesses of the leaflets are shown as the mean ± standard deviation. V0: (valve 0) uncrimped control; V1: (valve 1) calcified uncrimped; V2: (valve 2) calcified uncrimped; V3: (valve 3) calcified stent-crimped valve at 18-Fr; V4: (valve 4) calcified stent-crimped valve at 18-Fr; V5: (valve 5) calcified stent-crimped valve at 14-Fr; V6: (valve 6) calcified stent-crimped valve at 14-Fr.
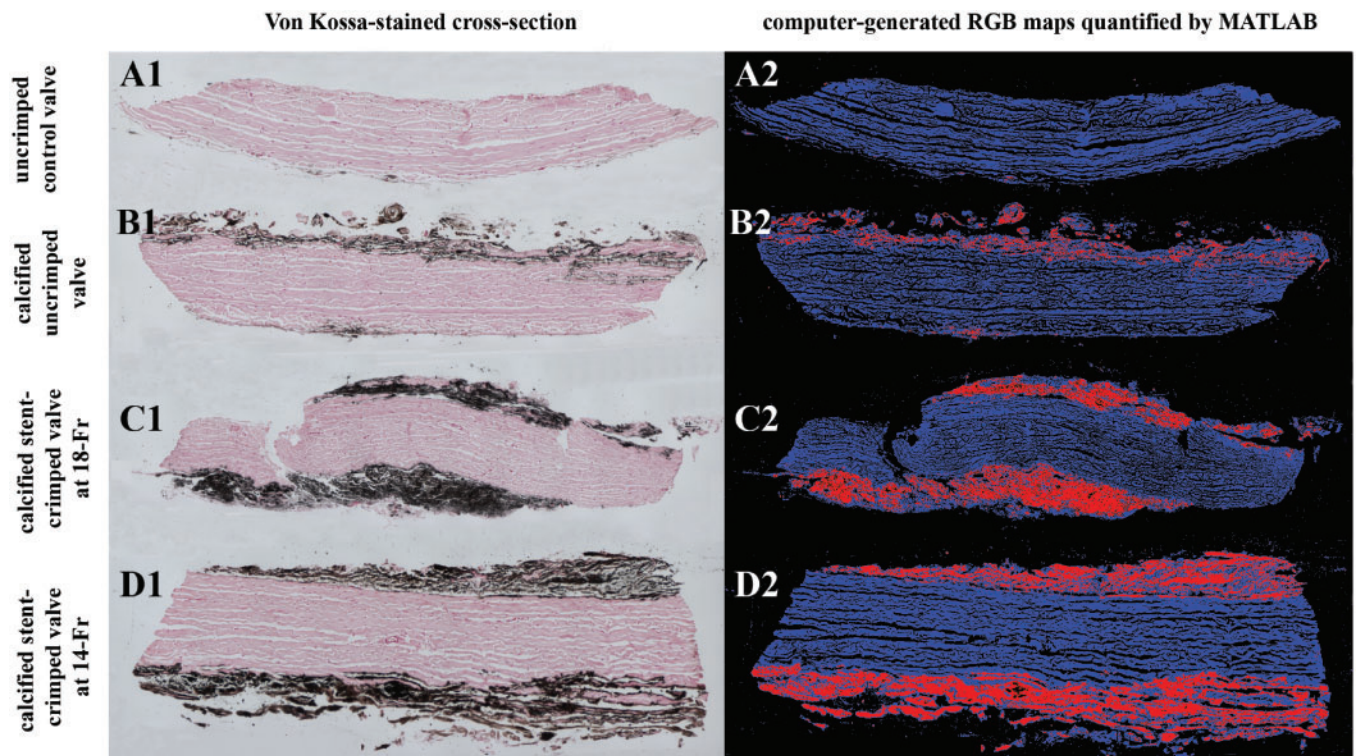

Figure 6: Von Kossa staining for quantifying calcification. The panels compare Von Kossa staining of representative samples of 4 different studied valve groups along with their computer-generated RGB map: a sample from the uncrimped control valve (**A1–2**); from a calcified uncrimped valve (**B1–2**); from a calcified stent-crimped valve at 18-Fr (**C1–2**); and from a calcified stent-crimped valve at 14-Fr (**D1–2**). A1, B1, C1 and D1 are Von Kossa-stained cross-sections of 4 different valves. Black regions demonstrate the calcification. A2, B2, C2 and D2 are computer-generated RGB maps quantified by an in-house MATLAB routine. Blue and red represent uncalcified and calcified regions, respectively. RGB: red, green and blue.
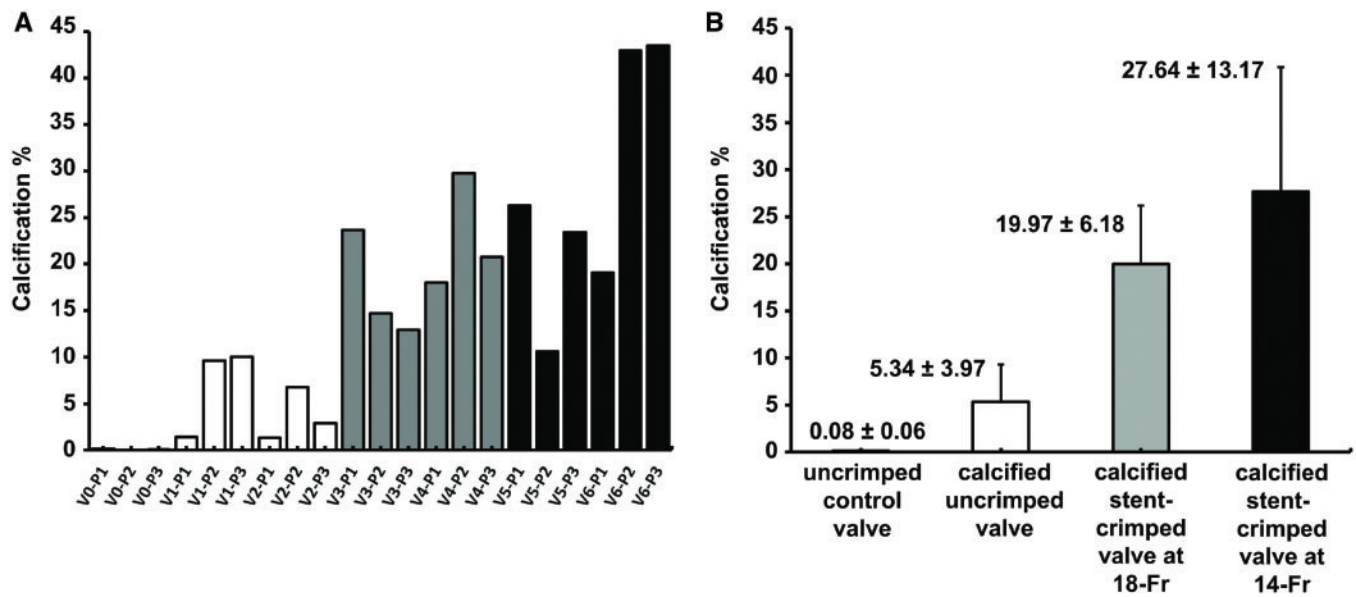
Figure 7: Quantification of calcified regions using histopathological analysis. (**A**) Total calcification ratio in terms of percentage quantified for each valve's post according to the computer analyses of the Von Kossa staining. (**B**) The average calcification in terms of percentage for all the valves' posts in each studied group is shown as mean ± standard deviation. V0: (valve 0) uncrimped control; V1: (valve 1) calcified uncrimped; V2: (valve 2) calcified uncrimped; V3: (valve 3) calcified stent-crimped valve at 18-Fr; V4: (valve 4) calcified stent-crimped valve at 18-Fr; V5: (valve 5) calcified stent-crimped valve at 14-Fr; V6: (valve 6) calcified stent-crimped valve at 14-Fr; P1, P2 and P3 denote valve posts 1, 2 and 3, respectively. Three punch biopsies were taken from each valve, adjacent to the valve's post.
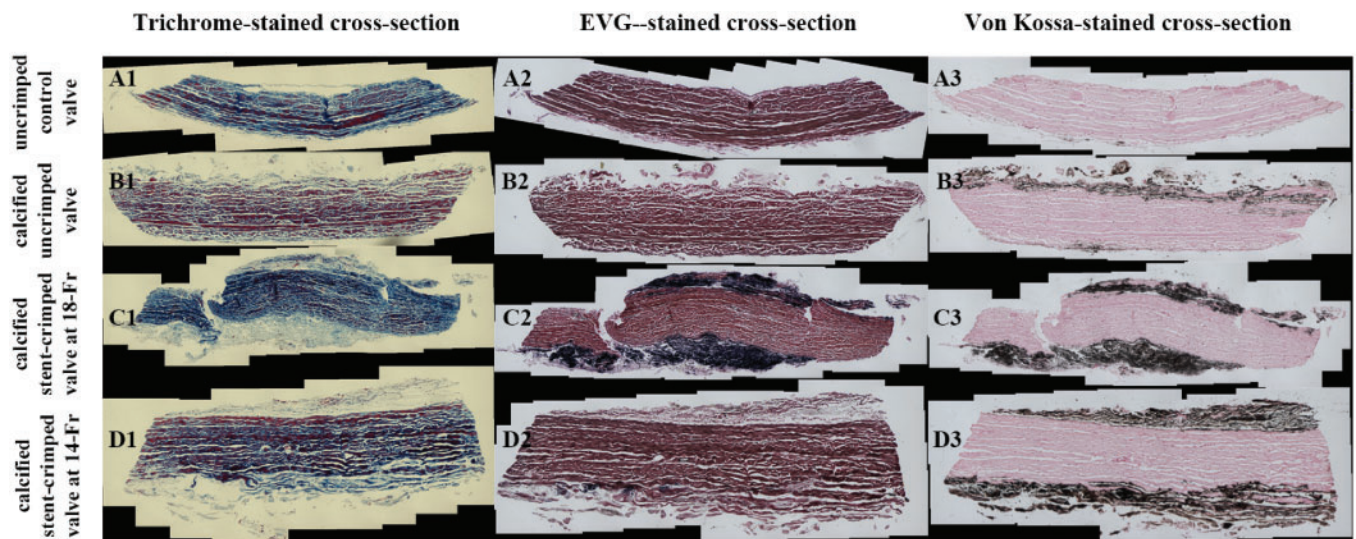

Figure 8: Association between the leaflet's extracellular matrix degeneration, elastin degradation and calcification. Trichrome (**A1–D1**), Elastic tissue fibres - Verhoeff-van Gieson (**A2–D2**) and Von Kossa staining (**A3–D3**) of the representative samples from each of the 4 studied groups: an uncrimped control valve (**A1–A3**); a calcified uncrimped valve (**B1–B3**); a calcified stent-crimped valve at 18-Fr; and (**C1–C3**) a calcified stent-crimped valve at 14-Fr (**D1–D3**). EVG: Elastic tissue fibres - Verhoeff's van Gieson.

cycles of exposure to a calcifying solution. This observation is interesting and, in our opinion, is associated with excessive calcium deposition in microscopic defects over the leaflets' ECM, which later on appears as calcification and structural valve degeneration [2, 22–24].

Stent-crimp-induced damage to the extracellular matrix and calcium depositions in the leaflets

Our histological results (Figs 6 and 8) suggest that calcium deposits were higher around the sutures and valve posts for all the

studied valves. These regions in a valve are usually under higher mechanical stress, and the ECM of these regions is therefore more prone to disruption [21], which may lead to calcification and early structural valve degeneration. We hypothesized that once the valve experiences stent crimping, the thin struts of the stent, with their very small surface area, amplify the crimping force into an enormous normal stress applied to the leaflets (like a cutting knife). This stress, which represents the external crimping force acting over the cross-sectional area of the leaflet, results in microscopic damage to the collagen fibres and elastin of the leaflets, as shown previously [25]. This stress may be responsible for remodelling the elastin and collagen fibres of the ECM of the

leaflets [26], which may increase the aggregation and deposition of calcium in the tissue [27–29]. Figures 6 and 8 illustrate the crimp-induced damage to the elastin and collagen fibrils of the leaflets. Other studies have also reported the damaging effects of stent crimping on valve leaflets [4, 6, 30]. Our durability data corroborate those of previous studies, indicating that stent crimping may damage the ECM of the leaflets [4, 6, 25, 30] and show for the first time that stent-crimped valves may be prone to further passive calcium deposits on their leaflets.

Accordingly, our observations showed that, in the uncrimped valves, only superficial layers of the leaflets were calcified. Nevertheless, in both 18-Fr and 14-Fr stent-crimped valves, the calcification penetrated the deeper layers of the tissue, which led to more calcium deposits compared to the uncrimped valves. Stent-crimp-induced damage to the ECM may allow calcium to penetrate more profoundly from the superficial layers down to the deeper layers (Figs 6 and 8). The influx of calcium into structurally damaged regions can result in calcium crystallization and lead to the potential growth of the microcalcification regions into clinically apparent calcium nodules on the leaflet.

Limitations

Because the standard AWT systems can accommodate only 6 valves at a time, the number of tested valves in this study was low, which prevents us from drawing any statistically significant conclusions. Therefore, we only emphasize the potential association between 2 observations, namely, stent crimping and the occurrence of calcification. Furthermore, the calcification reported in this study is passive and does not reflect the active, cellular-based calcification phenomenon that is present in the human heart. However, passive calcification tests are considered standard in heart valve research and development and are commonly used to test the tendency of a valve to become calcified [14, 16].

CONCLUSION

We conclude that more prominent calcified regions and damage to the ECM are observed near the posts of the stent-crimped valves compared to the uncrimped controls. Accordingly, the data suggest a potential association between stent crimping and calcification, which may explain the durability concerns associated with transcatheter aortic valves. Reduced durability and the potential for early degeneration are current concerns for the long-term treatment of patients with aortic valve disease. Additional larger studies are needed to better understand the effect of stent crimping and ultimately to improve the durability of transcatheter heart valves.

ACKNOWLEDGEMENTS

Funding

Conflict of interest: Arash Kheradvar is the founder of ValVention Inc., which aims to commercialize FoldaValve. He also has an equity interest in ValVention Inc., a company that may potentially benefit from the research results. The terms of this arrangement have been reviewed and approved by the University of California, Irvine in accordance with its conflict of interest policies. Danny Dvir is a cosultant to Edwards Lifesciences. All other authors declared no conflict of interest.

REFERENCES

[1] Leon MB, Smith CR, Mack MJ, Makkar RR, Svensson LG, Kodali SK et al. Transcatheter or surgical aortic-valve replacement in intermediate-risk patients. N Engl J Med 2016;374:1609–20.

[2] Dvir D, Bourguignon T, Otto CM, Hahn RT, Rosenhek R, Webb JG et al. Standardized definition of structural valve degeneration for surgical and transcatheter bioprosthetic aortic valves. Circulation 2018;137:388.

[3] Kheradvar A, Groves EM, Goergen CJ, Alavi SH, Tranquillo R, Simmons CA et al. Emerging trends in heart valve engineering: part II. Novel and standard technologies for aortic valve replacement. Ann Biomed Eng 2015;43:844–57.

[4] Zegdi R, Bruneval P, Blanchard D, Fabiani J-N. Evidence of leaflet injury during percutaneous aortic valve deployment. Eur J Cardiothorac Surg 2011;40:257–60.

[5] de Buhr W, Pfeifer S, Slotta-Huspenina J, Wintermantel E, Lutter G, Goetz WA. Impairment of pericardial leaflet structure from balloon-expanded valved stents. J Thorac Cardiovasc Surg 2012;143:1417–21.

[6] Kiefer P, Gruenwald F, Kempfert J, Aupperle H, Seeburger J, Mohr FW et al. Crimping may affect the durability of transcatheter valves: an experimental analysis. Ann Thorac Surg 2011;92:155–60.

[7] Ong SH, Mueller R, Iversen S. Early calcific degeneration of a CoreValve transcatheter aortic bioprosthesis. Eur Heart J 2012;33:586.

[8] Richardt D, Hanke T, Sievers HH. Two cases of heart failure after implantation of a CoreValve prosthesis. N Engl J Med 2015;372:1079–81.

[9] van Steenberghe M, de Vasconcelos C-Y, Delay D, Niclauss L, Kirsch M. Early transcatheter aortic valve degeneration in the young. Int J Cardiol 2016;222:786–7.

[10] Harbaoui B, Courand P-Y, Schmitt Z, Farhat F, Dauphin R, Lantelme P. Early Edwards SAPIEN valve degeneration after transcatheter aortic valve replacement. JACC Cardiovasc Interv 2016;9:198.

[11] Pascual I, Avanzas P, Morís C. Degenerative pattern of a percutaneous aortic valve. Rev Esp Cardiol (Engl Ed) 2017;70:772.

[12] Webb JG, Dvir D. Is transcatheter aortic valve replacement a durable therapeutic strategy? JACC Cardiovasc Interv 2015;8:1092.

[13] Deutsch M-A, Mayr NP, Assmann G, Will A, Krane M, Piazza N et al. Structural valve deterioration 4 years after transcatheter aortic valve replacement. Circulation 2015;131:682.

[14] Arora S, Ramm CJ, Misenheimer JA, Vavalle JP. Early transcatheter valve prosthesis degeneration and future ramifications. Cardiovasc Diagn Ther 2017;7:1–3.

[15] Makkar RR, Chakravarty T. Transcatheter aortic valve thrombosis: new problem, new insights. JACC Cardiovasc Interv 2017;10:698–700.

[16] Barannyk O, Fraser R, Oshkai P. A correlation between long-term in vitro dynamic calcification and abnormal flow patterns past bioprosthetic heart valves. J Biol Phys 2017;43:279–96.

[17] Kapolos J, Mavrilas D, Missirlis Y, Koutsoukos PG. Model experimental system for investigation of heart valve calcification in vitro. J Biomed Mater Res 1997;38:183–90.

[18] Kriegs M, Kanellopoulou D, Koutsoukos PG, Mavrilas D, Glasmacher B. Development of a new combined test setup for accelerated dynamic pH-controlled in vitro calcification of porcine heart valves. Int J Artif Organs 2009;32:794–801.

[19] Tertti R, Harmoinen A, Leskinen Y, Metsarinne KP, Saha H. Comparison of calcium phosphate product values using measurement of plasma total calcium and serum ionized calcium. Hemodialysis Int 2007;11:411–16.

[20] Mann HB, Whitney DR. On a test of whether one of two random variables is stochastically larger than the other. Ann Math Statist 1947;18:50–60.

[21] Alavi SH, Groves EM, Kheradvar A. The effects of transcatheter valve crimping on pericardial leaflets. Ann Thorac Surg 2014;97:1260–6.

[22] Otto CM. Calcification of bicuspid aortic valves. Heart 2002;88:321–2.

[23] Cheng CL, Chang HH, Huang PJ, Wang WC, Lin SY. Ex vivo assessment of valve thickness/calcification of patients with calcific aortic stenosis in relation to in vivo clinical outcomes. J Mech Behav Biomed Mater 2017; 74:324–32.

[24] Foroutan F, Guyatt GH, Otto CM, Siemieniuk RA, Schandelmaier S, Agoritsas T *et al.* Structural valve deterioration after transcatheter aortic valve implantation. Heart 2017;103:1899.

[25] Dasi LP, Hatoum H, Kheradvar A, Zareian R, Alavi SH, Sun W *et al.* On the mechanics of transcatheter aortic valve replacement. Ann Biomed Eng 2017;45:310–31.

[26] Delogne C, Lawford PV, Habesch SM, Carolan VA. Characterization of the calcification of cardiac valve bioprostheses by environmental scanning electron microscopy and vibrational spectroscopy. J Microsc 2007;228:62–77.

[27] Schoen FJ, Tsao JW, Levy RJ. Calcification of bovine pericardium used in cardiac valve bioprostheses. Implications for the mechanisms of bioprosthetic tissue mineralization. Am J Pathol 1986;123:134–45.

[28] Bertazzo S, Gentleman E, Cloyd KL, Chester AH, Yacoub MH, Stevens MM. Nano-analytical electron microscopy reveals fundamental insights into human cardiovascular tissue calcification. Nature Mater 2013;12: 576–83.

[29] Schoen FJ, Levy RJ. Calcification of tissue heart valve substitutes: progress toward understanding and prevention. Ann Thorac Surg 2005;79: 1072–80.

[30] Khoffi F, Heim F, Chakfe N, Lee JT. Transcatheter fiber heart valve: effect of crimping on material performances. J Biomed Mater Res B Res 2015; 103:1488–97.